SUPPLEMENTAL MATERIAL

RSPO2 Synergizes with BMP2 to Enhance Wnt-Dependent Bone Healing

Buchan Jiang[1,2], Erin B. Meymarian[1,3], Shije Shahin[1], Jack T. Wilkening[1], Alexander J. Knights[1,4,5], Archana Sanjay[6], Tristan Maerz[1,7], Yadav Wagley[1*], Kurt D. Hankenson[1,8*]

[1]Department of Orthopaedic Surgery, University of Michigan; Ann Arbor, MI, USA.

[2]Department of Orthopaedics, The Second Xiangya Hospital of Central South University; Changsha, Hunan, China.

[3]Department of Mechanical Engineering, University of Michigan; Ann Arbor, MI, USA.

[4]Department of Orthopaedic Surgery, Washington University; St Louis, MO, USA.

[5]Center of Regenerative Medicine, Washington University; St Louis, MO, USA.

[6]Department of Orthopaedics, Musculoskeletal Institute, School of Medicine, UConn Health; Farmington, CT, USA.

[7]Institute for Biomechanics, Department of Health Sciences and Technology, ETH Zürich; Zürich, Switzerland.

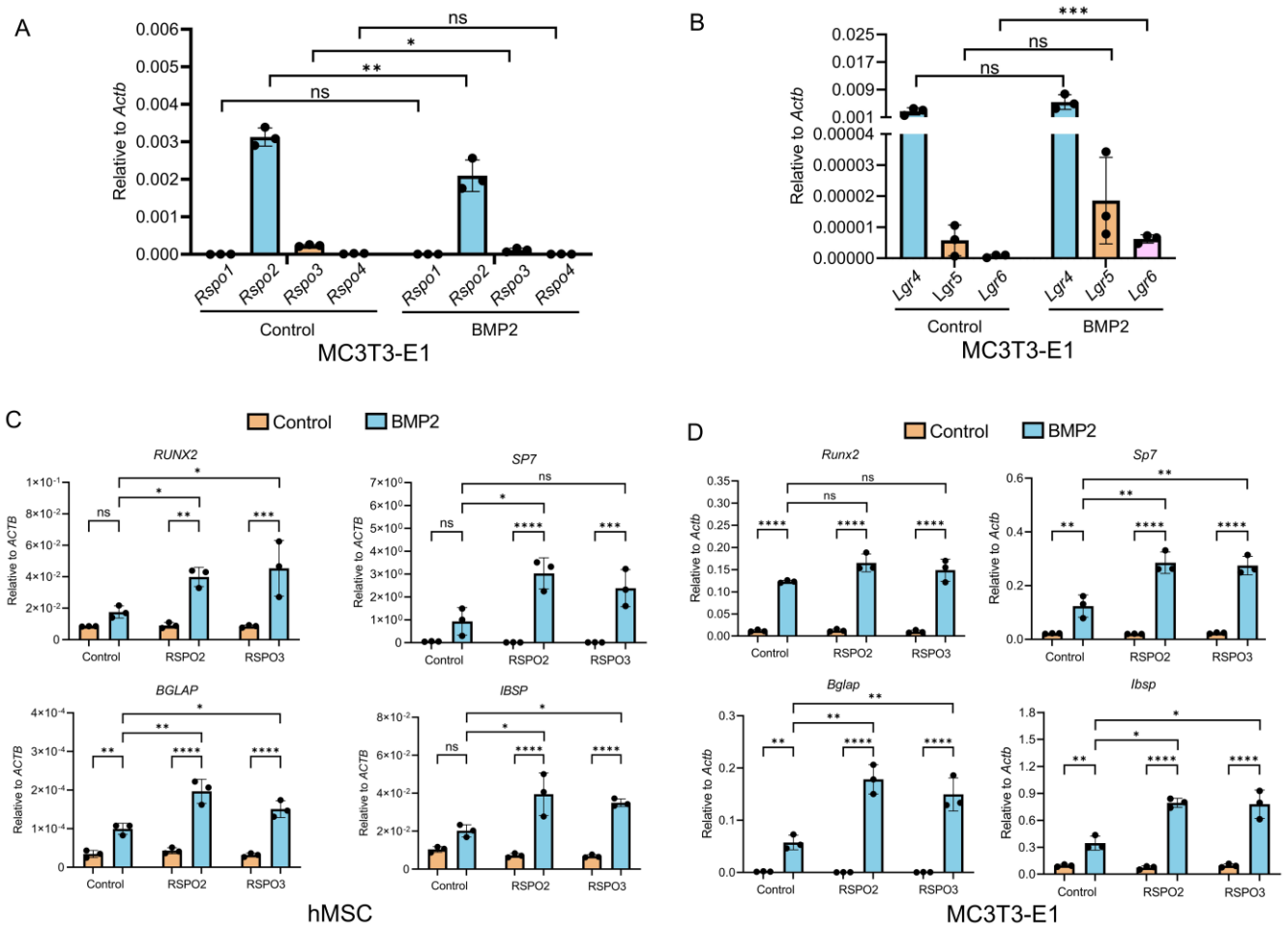
[8]Department of Biomedical Engineering and Department of Molecular and Integrative Physiology, University of Michigan; Ann Arbor, MI, USA.

*Corresponding authors

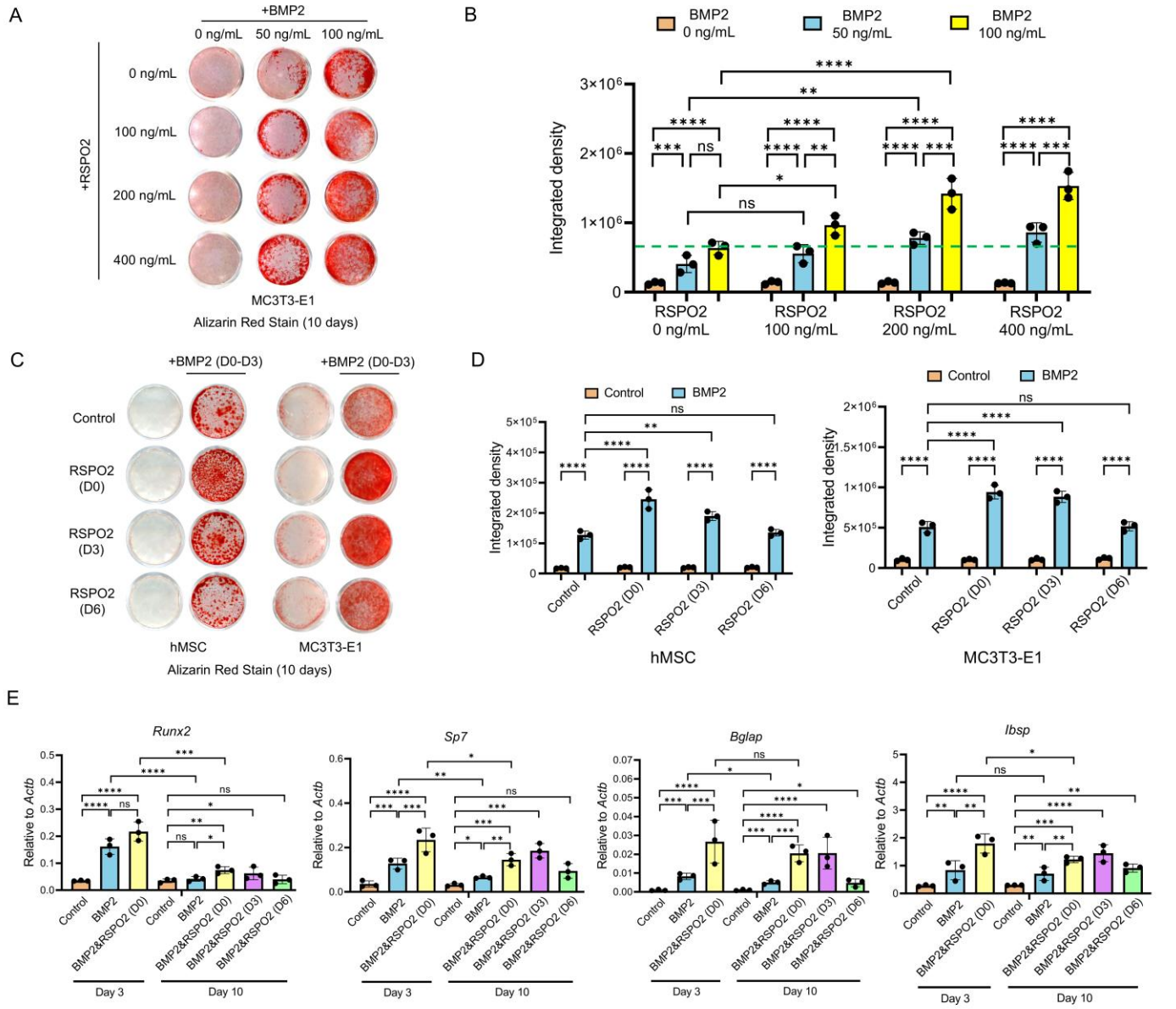
Supplemental Material:

Supplemental Figures 1-9

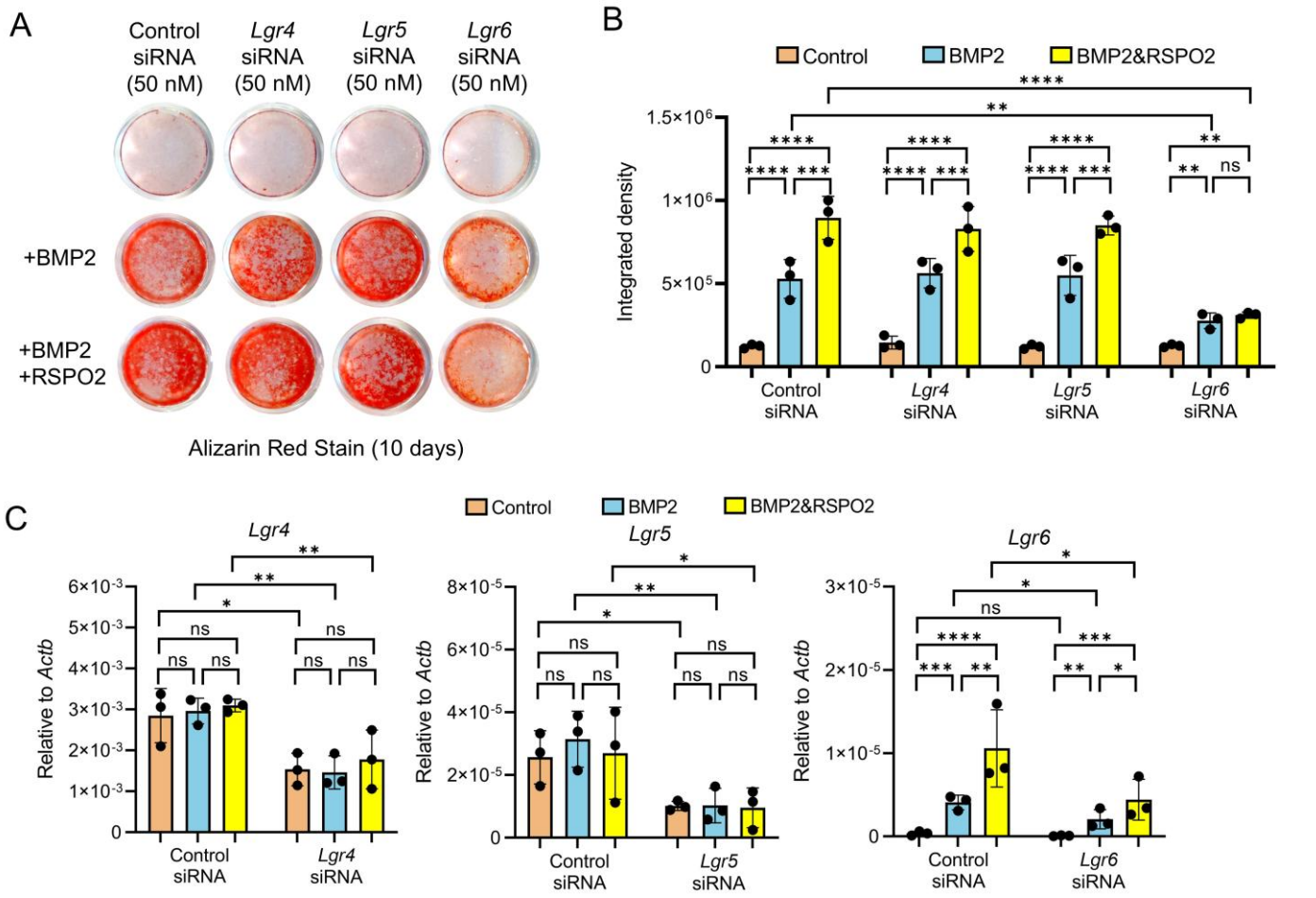
Supplemental Tables 1-2



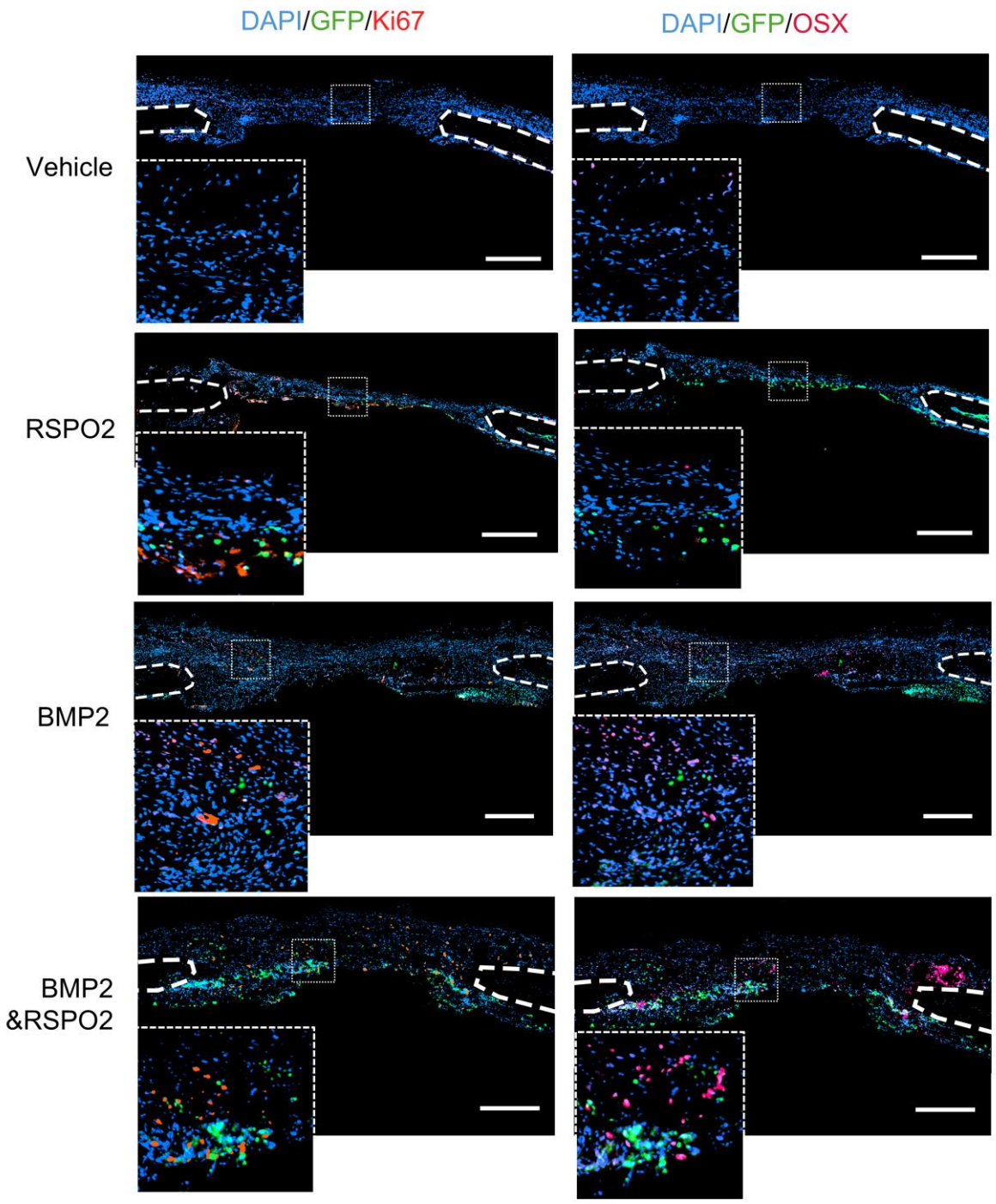
Supplemental Figure 1. Cross-talk between RSPO and BMP2 signaling promotes osteogenic marker expression. **(A)** Expression of *Rspo1/2/3/4* and **(B)** *Lgr4/5/6* in the MC3T3-E1 cell line were determined after BMP2 (100 ng/mL) stimulation for three days in osteo-permissive media. **(C)** mRNA expression of osteoblast marker genes was measured via qPCR in hMSCs and **(D)** MC3T3-E1 cells stimulated with BMP2 (200 ng/mL and 100 ng/mL, respectively) in the presence or absence of RSPO2 (200 ng/mL) or RSPO3 (200 ng/mL) for 5 days, as indicated. Orange bar: control group; blue bar: BMP2 treatment group. Three independent donors were used for hMSCs, and MC3T3-E1 experiments were independently repeated three times. Data were analyzed by two-way ANOVA and Tukey's multiple comparisons test; data are shown as mean ± SD; ns, not significant; *, $P < 0.05$; **, $P < 0.01$; ***, $P < 0.001$; ****, $P < 0.0001$.



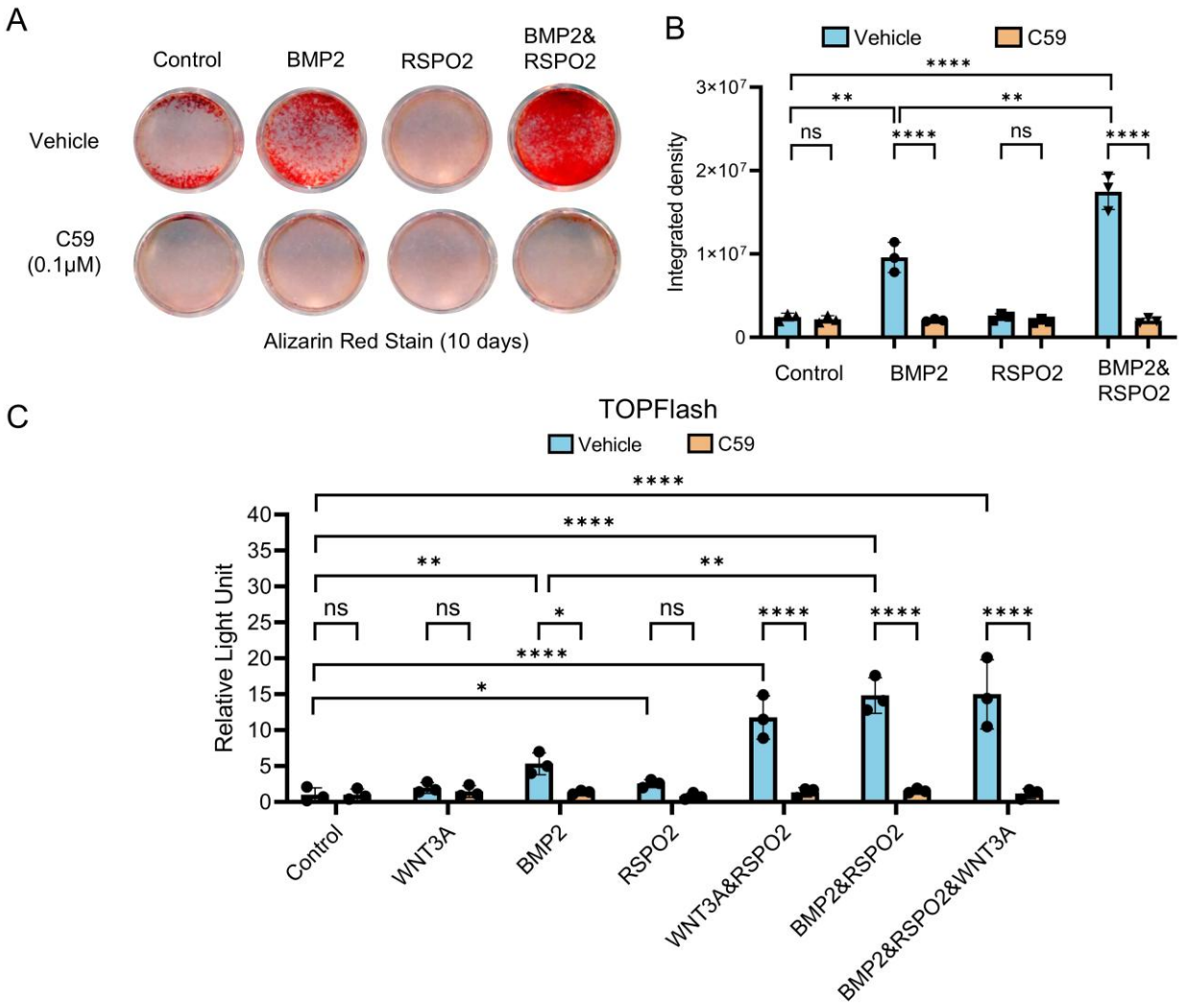
Supplemental Figure 2. RSPO2 promotes BMP2-induced osteogenesis in a dose- and time-dependent manner. **(A)** Representative Alizarin Red S staining (10 days) of MC3T3-E1 cells stimulated with suboptimal (50 ng/mL) or standard (100 ng/mL) doses of BMP2 and a range of RSPO2 concentrations (100, 200, and 400 ng/mL); the mineralization density was quantified, shown in **(B)**. The green horizontal dashed line in **(B)** represents the average value of the standard BMP2-only group as a benchmark. **(C)** Representative Alizarin red S stain (10 days) of a hMSC donor line and MC3T3-E1 cells stimulated with BMP2 (200 ng/mL and 100 ng/mL, respectively) and treated with RSPO2 (200 ng/mL) at the indicated time points; RSPO2 was added either at the same time as BMP2 (D0), or 3 days (D3) or 6 days (D6) after BMP2 treatment; the mineralization density was quantified, shown in **(D)**. **(E)** mRNA expression levels of osteogenic marker genes in MC3T3-E1 cells. Cells were stimulated with BMP2 (100 ng/mL) for 3 or 10 days. For the 10-day experiment, cells treated with BMP2 were additionally treated with RSPO2 (200 ng/mL) either concurrently with BMP2 (D0), or at 3 (D3) or 6 (D6) days post-BMP2 treatment. Data from three independent hMSC donors were utilized, and the MC3T3-E1 experiments were independently replicated three times. Data were analyzed by two-way ANOVA and Tukey's multiple comparisons test; data are shown as mean ± SD; ns, not significant; *, $P < 0.05$; **, $P < 0.01$; ***, $P < 0.001$; ****, $P < 0.0001$.



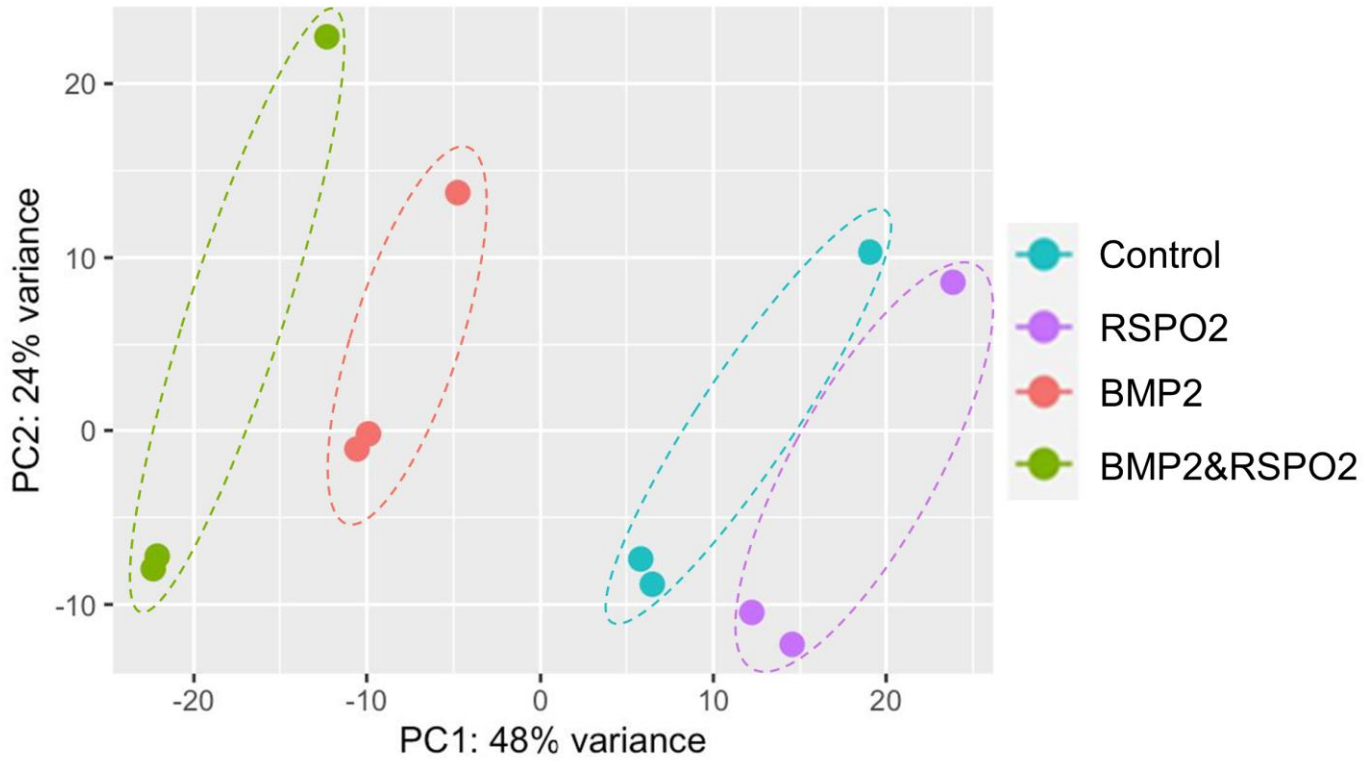
Supplemental Figure 3. siRNA-mediated LGR6 silencing impaired BMP2-induced mineralization and attenuated RSPO2-induced synergistic effects. (A) MC3T3-E1 cells transfected with *Lgr4*, *Lgr5*, or *Lgr6* siRNA or scrambled siRNA (control siRNA) at 50 nM in the presence or absence of BMP2 (100 ng/mL) and RSPO2 (200 ng/mL); **(B)** quantitative image analysis was used to quantify the relative mineralization, and **(C)** knockdown efficiency was confirmed by measuring Lgr4, Lgr5, and Lgr6 mRNA expression on day 3, which showed approximately 60%, 70%, and 60% reductions, respectively, relative to scrambled siRNA controls. Data were analyzed by two-way ANOVA and Tukey's multiple comparisons test; data are shown as mean ± SD of 3 independent experiments; ns, not significant; *, $P < 0.05$; **, $P < 0.01$; ***, $P < 0.001$; ****, $P < 0.0001$.



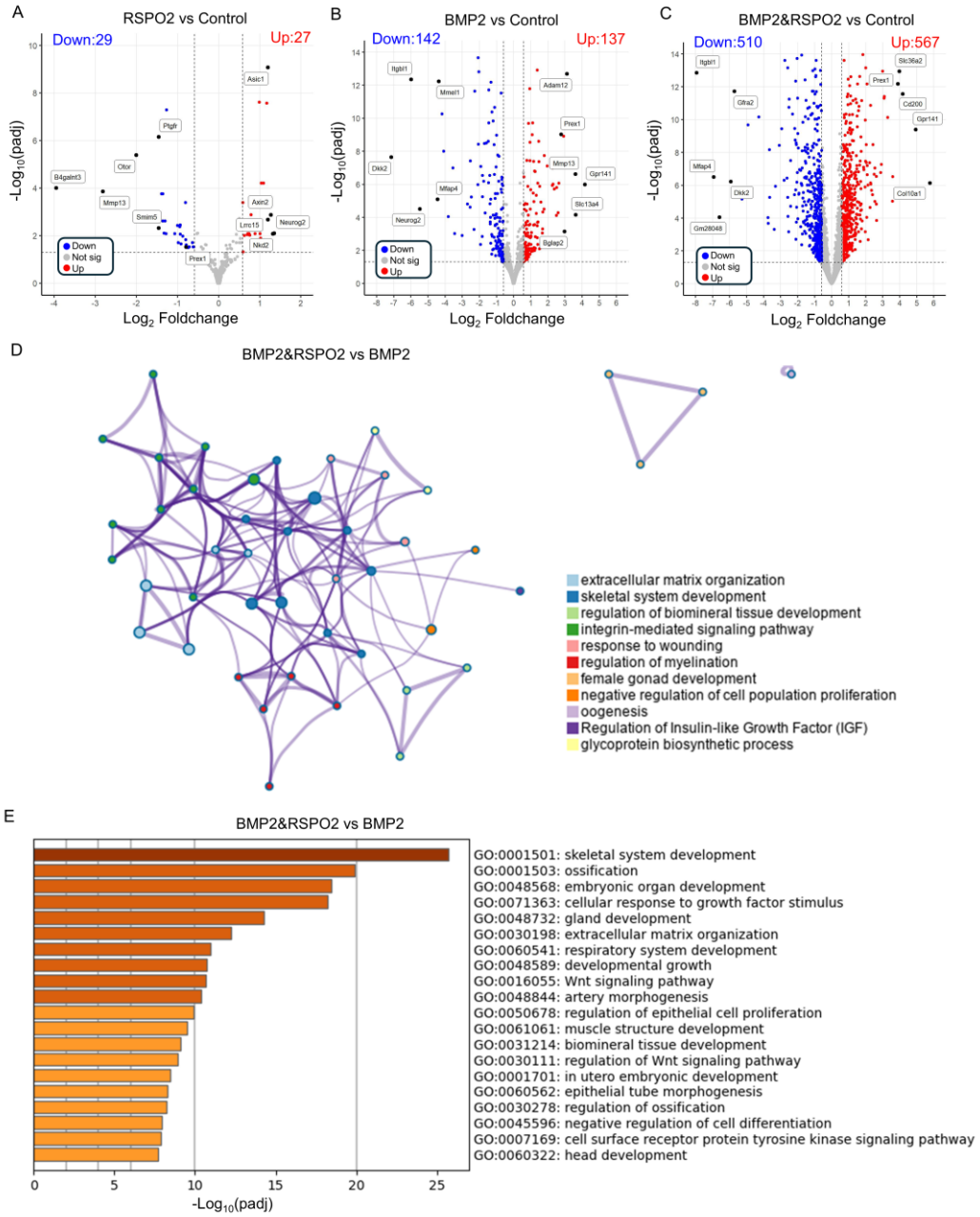
Supplemental Figure 4. Co-localization of GFP with Ki67 and Osterix in TCF/Lef:H2B-GFP calvarial defects. Representative merged immunofluorescence images from calvarial defects harvested 10 days after treatment with vehicle, RSPO2 (1 μg), BMP2 (0.25 μg), or BMP2+RSPO2. Left panels show DAPI, GFP, and Ki67 staining used for quantification of proliferating Wnt-responsive cells (GFP^+Ki67^+). Right panels show DAPI, GFP, and Osterix (OSX) staining used for quantification of osteogenic Wnt-responsive cells (GFP^+OSX^+). Scale bars = 400 μm. Dashed line: margin of calvaria bone.



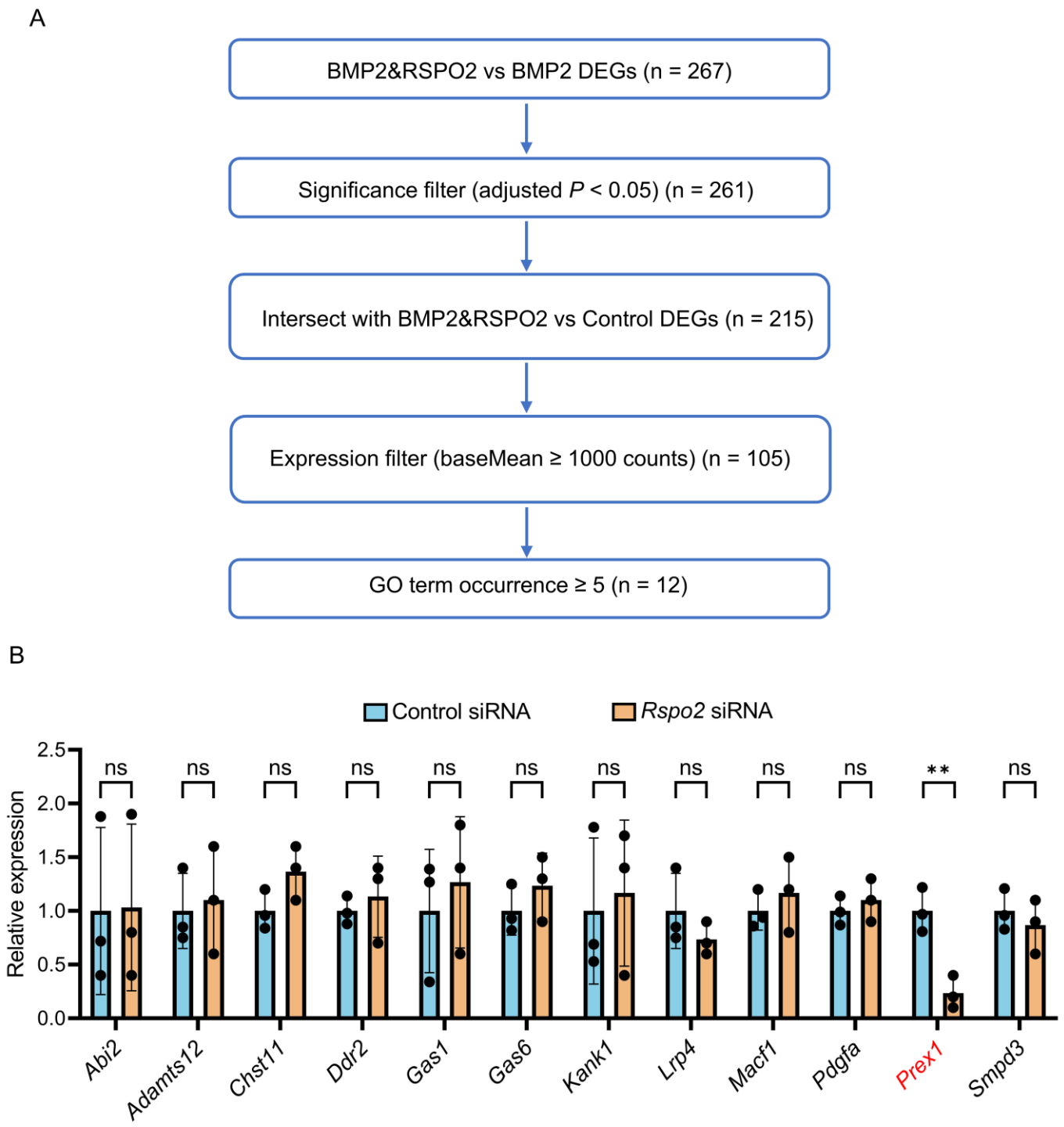
Supplemental Figure 5. Active Wnt signaling by Wnts secreted during the early phase of differentiation is required for BMP2-induced osteogenesis. (A) Alizarin red S stain (10 days) of MC3T3-E1 cells treated in the presence or absence of Wnt secretion inhibitor C59 (0.1 μM), BMP2 (100 ng/mL), and/or RSPO2 (200 ng/mL), as indicated. C59 was added for the first 3 days; and **(B)** the mineralization density from 3 representative plates was quantified using quantitative image analysis. **(C)** Luciferase assay of MC3T3-E1 cells transduced with a TCF/LEF-responsive TOPFlash reporter (Firefly luciferase driven by multimerized TCF/LEF binding sites) demonstrates that BMP2-RSPO2 co-treatment increases Wnt/β-catenin pathway activation, comparable to WNT3A (200 ng/mL) and RSPO2 (200 ng/mL) co-treatment within 3 days. Pretreatment with C59 (0.1 μM) completely abrogated this luciferase response. Three independent experiments were performed. Data were analyzed by two-way ANOVA and Tukey's multiple comparisons test; data are shown as mean ± SD of 3 independent experiments; ns, not significant; *, $P < 0.05$; **, $P < 0.01$; ***, $P < 0.001$; ****, $P < 0.0001$.



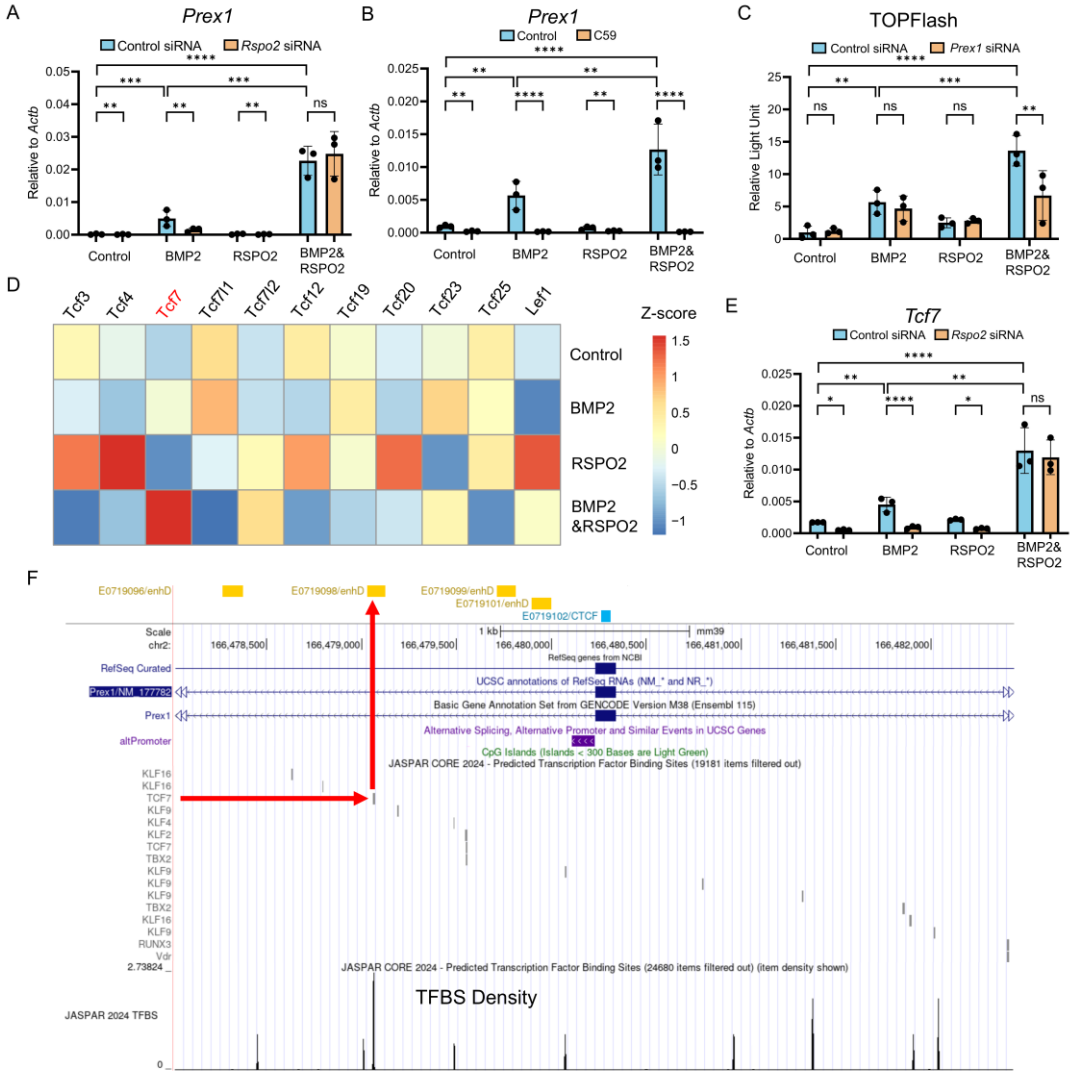
Supplemental Figure 6. Principal-component analysis (PCA) showing distinct positions of the bulk RNA sequencing (RNA-seq) samples. The PCA figure represents a two-dimensional scatterplot of the first two principal components of the RNA-Seq data. PC1 and PC2 explained 48% and 24% of the total variance, respectively. The four sample groups are represented by different colors as indicated by the legend provided within the graph. Each dot represents an independent experiment of an RNA-Seq sample.



Supplemental Figure 7. RNA-seq revealed differentially expressed genes and enriched pathways. Volcano plot of significantly differentially expressed genes (DEGs) (Fold change ≥ 1.5, adjusted *P* value < 0.05) in the **(A)** RSPO2-only, **(B)** BMP2-only, **(C)** BMP2-RSPO2 co-treatment group in comparison with control group. Blue dots represent downregulated genes, gray dots represent non-significant genes, and red dots represent upregulated genes. The top five genes with the highest or lowest fold change are labeled. **(D)** Enriched ontology cluster analysis for BMP2-RSPO2 co-treatment vs BMP2 alone using Metascape shows the enriched GO terms colored by cluster identity, where nodes that share the same cluster identity are typically close to each other. **(E)** Functional pathway enrichment analysis using Metascape, showing the top GO pathways in the comparison between BMP2 and RSPO2 co-treatment and BMP2-only treatment ranked by $-\log_{10}$(adjusted *P* value).



Supplemental Figure 8. Stepwise prioritization of candidate mediators of BMP2–RSPO2 synergy. (A) DEGs were first identified from the BMP2-RSPO2 co-treatment versus BMP2 comparison and then intersected with DEGs from the BMP2 and RSPO2 co-treatment versus control comparison. Subsequent filtering based on transcript abundance (basemean ≥ 1000 counts) and functional breadth (≥ 5 enriched PANTHER GO biological process terms) yielded a final set of 12 high-priority genes, including *Prex1*. **(B)** *Rspo2* knockdown screen identified *Prex1* as the dominant RSPO2-dependent target. Relative mRNA expression levels of the 12 high-confidence genes in MC3T3-E1 cells in the presence or absence of *Rspo2* siRNA (50 nM), as indicated. RNA samples were obtained 5 days after siRNA treatment. Data were analyzed using unpaired two-tailed Student's *t* tests; data are shown as mean ± SD of 3 independent experiments; ns, not significant; *, $P < 0.05$; **, $P < 0.01$; ***, $P < 0.001$; ****, $P < 0.0001$.



Supplemental Figure 9. Evidence supporting a TCF7–PREX1 transcriptional axis downstream of BMP2-RSPO2 signaling. (A) Relative mRNA expression level of *Prex1* in MC3T3-E1 cells in the presence or absence of *Rspo2* siRNA (50 nM), BMP2 (100 ng/mL), and/or RSPO2 (200 ng/mL), as indicated. RNA samples were obtained 5 days after the initial treatment. **(B)** mRNA expression level of *Prex1* was determined in MC3T3-E1 cells in the presence or absence of Wnt secretion inhibitor C59 (0.1 μM), BMP2 (100 ng/mL), and/or RSPO2 (200 ng/mL), as indicated. C59 was added for the first 3 days and RNA samples were obtained 5 days after the initial treatment. **(C)** TOPFlash assay of MC3T3-E1 cells shows that siRNA (80 nM) -mediated *Prex1* knockdown reversed the increase in Wnt activity induced by BMP2 and RSPO2 co-treatment versus BMP2-only treatment. Cells were left for 48 hours after BMP2/RSPO2 stimulation before luciferase assays were performed. **(D)** Heatmap showing z-score-normalized expression of all detectable *Tcf* and *Lef* family members across control, BMP2, RSPO2, and BMP2+RSPO2 conditions from RNA-seq data. Among these factors, *Tcf7* is the only family member significantly upregulated in the BMP2 and RSPO2 co-treatment group compared to the BMP2-only treatment group. **(E)** Relative expression levels of *Tcf7* in MC3T3-E1 cells transfected with *Rspo2* siRNA (50 nM) or control siRNA in the presence or absence of BMP2 (100 ng/mL) and RSPO2 (200 ng/mL). **(F)** Transcription factor binding site (TFBS) analysis using UCSC Genome browser predicted a potential TCF7-binding site within a distal enhancer of the *Prex1* gene with a relatively high TFBS density. The red arrow indicates the predicted enhancer region (yellow). Data in graphs were analyzed by two-way ANOVA and Tukey's multiple comparisons test; data are shown as mean ± SD of 3 independent experiments; ns, not significant; *, $P < 0.05$; **, $P < 0.01$; ***, $P < 0.001$; ****, $P < 0.0001$.

Supplemental Table 1. Quantitative reverse transcription polymerase chain reaction (RT-qPCR) primers.

Species	Gene	Forward	Reverse
Human	*ACTB*	5′-CGGCGCCCTATAAAACCCA	5′-CGCGGCGATATCATCATCCA
Human	*RSPO1*	5′-GATTGAGCAACTTGGGAACGG	5′-GAAACCACAATCTCAGCTTCG
Human	*RSPO2*	5′-ACACCGAGCCCCAGATATGA	5′-ACCAACTTCACATCCTTCCAC
Human	*RSPO3*	5′-TAGTCAAGGCTGCCAAGGAG	5′-TCACAGTCAGCTTTGCATTTTGT
Human	*RSPO4*	5′-AAATGTGGGGCCACTTGTGA	5′-CAGTTCACACTCCCCCTGG
Human	*LGR4*	5′-CCAAGCGCTGGATATCAGTATG	5′-CCCGCCAATTGTAGCTCTTC
Human	*LGR5*	5′-GTCTTCACCTCCTACCTAGACCT	5′-GTTAGCATCCAGACGCAGGG
Human	*LGR6*	5′-TAACCCAATCCAGTTTGTGGGAA	5′-GCAGCTCCTCAATTTGATTGTGA
Human	*RUNX2*	5′-ATAGCGTGCTGCCATTCGAG	5′-GTATGTCCGCCACCACTCAC
Human	*SP7*	5′-GCTTGAGGAGGAAGTTCACTAT	5′-GCTTCTTTGTGCCTGCTTTG
Human	*BGLAP*	5′-CTCACACTCCTCGCCCTATTG	5′-CTTGGACACAAAGGCTGCAC
Human	*IBSP*	5′-ACAACACTGGGCTATGGAGA	5′-CCTTGTTCGTTTTCATCCAC
Mouse	*Actb*	5′-TGGCATAGAGGTCTTTACGG	5′-AAGAGCTATGAGCTGCCTGA
Mouse	*Rspo1*	5′-GATCAAGGGCAAGAGACAGA	5′-GTTCCTCTCCAGCAGAATGA
Mouse	*Rspo2*	5′-CGTGTAGCAGAAACAACCGCAC	5′-GAAGACGCTGTGCTGCTCTTG
Mouse	*Rspo3*	5′-ACACCTTGGAAAGTGCCTTGA	5′-TGGCCTCACAGTGTACAATACT
Mouse	*Rspo4*	5′-CGAGTTGCCGAGTGTTATCT	5′-TCCAACTTCCTGTCCTTACG
Mouse	*Lgr4*	5′-CCTTCACCCAAGCACTGGATA	5′-AGGTCGTTACCAGCCAGTTG
Mouse	*Lgr5*	5′-AGCCTCGTGGTTCTGCATC	5′-GTGTCTTGATTGCAGTGGGG
Mouse	*Lgr6*	5′-TTGCGCTGTGCTGTGCG	5′-GGTTGTTCATACTGAGGTCTAGGT
Mouse	*Alpl*	5′-TGTGTGGGGTGAAGGCCAAT	5′-TCGTGGTGGTCACAATGCCC
Mouse	*Ibsp*	5′-AAAGTGAAGGAAAGCGACGA	5′-GTTCCTTCTGCACCTGCTTC
Mouse	*Bglap*	5′-CACCATGAGAGCCCTCACACTC	5′-CCTGCTTGGACACAAAGGCTG
Mouse	*Runx2*	5′-CCACCACTCACTACCACACG	5′-CACTCTGGCTTTGGGAAGAG
Mouse	*Axin2*	5′-ATGTCCTGTCTGCCAGCGTTC	5′-CAAGCACTAGCCAGTGGGTCAA
Mouse	*Gfp*	5′-GACGACGGCAACTACAAGAC	5′-TCGGCCATGATATAGACGTT
Mouse	*Id1*	5′-CTCTACGACATGAACGGCTGT	5′-TGCTCACCTTGCGGTTCTG
Mouse	*Sp7*	5′-GATGGCGTCCTCTCTGCTTG	5′-GCCATAGTGAGCTTCTTCCTCAA
Mouse	*Prex1*	5′-ATGTTCACTTGGAGCACGGT	5′-AAGGCCTCAAGGATCTTGGC
Mouse	*Tcf7*	5′-AGGTGGCATGCACTATCTCG	5′-TGCATTTCTTTTTCCTCCTGTGG

Supplemental Table 2. Quality control of RNA-seq data.

Sample	Total raw reads	Total valid reads	Valid Ratio%	Mapped reads	Mapped%	Q30%	GC%	RIN
Control_1	41607234	40138026	96.47	29809469	74.27%	98.36	51	10
Control_2	52178842	50351858	96.5	40282290	80.00%	98.25	51	10
Control_3	52971714	50914864	96.12	39172875	76.94%	98.24	51	10
RSPO2_1	51760980	50036974	96.67	39497693	78.94%	98.29	50	10
RSPO2_2	49873158	48212860	96.67	37875933	78.56%	98.18	51	10
RSPO2_3	53085458	51173798	96.4	29901202	58.43%	98.32	54	10
BMP2_1	34196646	32928102	96.29	23634682	71.78%	98.18	51	10
BMP2_2	47430328	45668508	96.29	37211409	81.48%	98.11	50	10
BMP2_3	46231024	44594678	96.46	35926265	80.56%	98.11	50	10
BMP2&RSPO2_1	41458452	36756910	88.66	16094797	43.79%	98.43	55	10
BMP2&RSPO2_2	48580434	46645164	96.02	36687413	78.65%	98.11	51	10
BMP2&RSPO2_3	48221124	46192532	95.79	36438558	78.88%	98.1	51	10